dividual local oscillator offsets thus compensate for this differential Doppler shift, as well as for the common corrections due to the earth's orbital motion and the motion of the sun with respect to the local standard of rest.

Observations were conducted from 8 to 12 June 1967. Observing bandwidths of either 6 or 120 khz were used, and a variety of OH-emission sources were observed. Circularly polarized feeds were used on both antennas, and either sense of polarization could be selected. The reductions completed so far have concentrated on the strongest feature in the 1665 Mhz spectrum of W3. This line has a radial velocity of −45.1 km per second with respect to the local standard of rest and is strongest when right, circularly polarized radiation is received. The 6-khz bandwidth is wide enough to display the complete line profile, and the presence of the line on each computer tape was easily verified by taking the Fourier transform of the autocorrelation function for each set of data.

The fringe phase and amplitude of the interferometric combination was derived by the method outlined by Rogers (*8*). The recorded video signals were cross-correlated at delay intervals (τ) centered on the expected geometric time delay for the observed source. The cross-correlation function was taken over periods of 0.02 second, which was short compared to the apparent fringe period. The time dependence of the cross-correlation function was removed through multiplication by a trial function, equivalent to a local oscillator offset. This operation, when the trial function is correctly chosen, converts the cross-correlation function to a time-independent function, $R(\tau)$; the fringe amplitude and phase can be derived as a function of frequency from the complex Fourier transform. The apparent local oscillator offset can be caused by a real difference between the two frequency standards or by an error in the adopted base line. The two effects can be separated by observation of the diurnal variation of the frequency offset. An incorrect frequency offset diminishes the apparent fringe visibility; therefore, a range of offsets was covered to make certain that the fringe visibility was maximized.

From the examples of the computer output (Fig. 1), it is clear that the offset can be determined to better than 0.01 hertz. This corresponds to an accuracy of six parts in 10^{12} in measuring the apparent frequency difference, and with sufficiently long integration the accuracy could be significantly improved. Over the 4-day observing period, the offset correction varied less than 0.1 hertz. The fringe visibility was derived from taking autocorrelation spectra of each record and comparing the observed fringe amplitude with the expected value.

The line of W3 at −45.1 km per second was observed over an hour-angle range of 14 hours, and the fringe visibility is 1.0 ± 0.2 over the entire range. We can find no evidence of resolving the source, thus implying an upper limit to the apparent size of 0.02 second of arc, for the equivalent uniform disk. If the apparent size refers to the true size of the OH source, its linear dimension would be less than 34 astronomical units at a distance of 1700 parsec for W3.

In addition to the scientific potentiality, the method promises to be a powerful technique in checking frequency standards and clocks. The best timing accuracy can be achieved with the widest bandwidths; however, the narrow bandwidth of the OH lines aids greatly in establishing the first timing estimates, in view of the fact that millisecond timing is sufficiently good as a first approximation. Successively better approximation can then be made by widening the bandwidth to include lines at other velocities. The OH lines of W3 are sufficiently strong to permit the use of smaller antennas for such timing applications, and a dish diameter of 9 m should be adequate.

J. M. MORAN, P. P. CROWTHER
Research Laboratory of Electronics, Massachusetts Institute of Technology, Cambridge, Massachusetts 02139

B. F. BURKE, A. H. BARRETT
Department of Physics and Research Laboratory of Electronics, Massachusetts Institute of Technology

A. E. E. ROGERS, J. A. BALL
J. C. CARTER
Lincoln Laboratory, Massachusetts Institute of Technology

C. C. BARE
National Radio Astronomy Observatory Green Bank, West Virginia

References and Notes

1. S. Weinreb, M. L. Meeks, J. C. Carter, A. H. Barrett, A. E. E. Rogers, *Nature* **208**, 440 (1965); A. H. Barrett and A. E. E. Rogers, *ibid.* **210**, 188 (1966); R. D. Davies, G. de Jager, G. L. Verschuur, *ibid.* **209**, 974 (1966).
2. A. E. E. Rogers, J. M. Moran, P. P. Crowther, B. F. Burke, M. L. Meeks, J. A. Ball, G. M. Hyde, *Phys. Rev. Lett.* **17**, 450 (1966); D. D. Cudaback, R. B. Read, G. W. Rougoor, *ibid.*, p. 452; A. E. E. Rogers, J. M. Moran, P. P. Crowther, B. F. Burke, M. L. Meeks, J. A. Ball, G. M. Hyde, *Astrophys. J.* **147**, 369 (1967).
3. J. M. Moran, A. H. Barrett, A. E. E. Rogers, B. F. Burke, B. Zuckerman, H. Penfield, M. L. Meeks, *Astrophys. J.* **148**, L69 (1967).
4. R. D. Davies, B. Rowson, R. S. Booth, A. J. Cooper, H. Gent, R. L. Adgie, J. H. Crowther, *Nature*, in press.
5. N. W. Broten, T. H. Legg, J. L. Locke, C. W. McLeish, R. S. Richards, R. M. Chisholm, H. P. Gush, J. L. Yen, J. A. Galt, *Science* **156**, 1592 (1967).
6. C. Bare, B. G. Clark, K. I. Kellerman, M. H. Cohen, D. L. Jauncey, *ibid.*, in press.
7. Hydrogen frequency standard, Varian Model H-10; rubidium frequency standard, Varian Model R-20.
8. A. E. E. Rogers, *Technical Report 457*, Research Laboratory of Electronics (Massachusetts Institute of Technology, Cambridge, 1967).
9. We thank G. M. Hyde, who provided time and frequency standards at the Haystack Facility (HF); N. M. Brenner for assistance with the programming at HF; the staff of the computation center of HF, where data reduction was carried out; the observing staffs of both the NRAO and HF; T. L. Wilson for help in making the observations; and S. Weinreb, D. S. Heeschen, M. L. Meeks, and P. B. Sebring for encouragement. Supported in part by NASA (grant NsG-419) and by NSF (grant GP-7046). Lincoln Laboratory is operated by M.I.T. with the support of the U.S. Air Force; NRAO is operated by Associated Universities, Inc., under contract with NSF.

28 June 1967

Bermuda's Southern Aeolianite Reef Tract

Abstract. *The outer reef on the explored southeast margin of the Bermuda platform is a submerged dune ridge thinly veneered with encrusting organisms. Aeolianites were deposited on what appears to be an older truncated surface, the reef-front terrace, now submerged to a depth of about 18 meters. Underwater examination reveals relict features of probable solutional origin that honeycomb the aeolinite and that have undergone only minor modification by erosion since the last eustatic rise of the sea. Submarine planation, even in this marginal area of reef growth, is a relatively slow process.*

The Bermuda platform, bounded by 32°14′ and 32°29′N and 64°37′ and 65°00′W, is located at the northern limit of reef growth in the North Atlantic Ocean. Conditions for reef development are now marginal (winter temperatures drop to about 18°C); a drop of only several degrees for a short continuous period would terminate the present sparse growth of corals and related reef organisms (*1, 2*).

Thus it is not surprising that climatic fluctuations there during the glacial epochs and more recently have resulted in intermittent growth of reef. This discontinuous buildup of the carbonate cap on an essentially tectonically stable platform (3) makes Bermuda a strategic reference point for the measurement of Pleistocene-to-Recent changes in sea level in this part of the world. We now call attention to some peculiarities of Bermuda reefs that bear on the problem of eustatic variation and recent history of this oceanic platform.

Most geologic studies of Bermuda (3-5) have attempted to interpret Pleistocene conditions on the basis of the stratigraphy and morphology of the exposed rocks making up the fishhook-like chain of Bermuda islands. Approximately 150 islands and islets cover less than 10 percent of the total surface of the Bermuda platform, a shallowly submerged elliptical area covering about 650 km². The platform, trending NE-SW, is essentially a carbonate cap surmounting a volcanic cone. An early coring (6) recovered basaltic lavas from 74 m below the present sea level.

Little is known about the morphology and origin of the submerged carbonate platform, an area that records much of the history of recent Bermuda; it (Fig. 1) includes (i) depressions within the islands (enclosed, such as Harrington Sound; semi-enclosed, such as Castle Harbor), (ii) shallow lagoonal areas enclosed within the ellipse of the outer reef, (iii) a broad reef-front terrace (referred to by fishermen as "broken ground") extending seaward of the reef tract to the outer margin of the platform, and (iv) the reefs proper.

The reef-front terrace, essentially a broad, slightly irregular surface submerged 8 to 10 fathoms (14 to 18 m), ranges from 1 to about 7 km in width [Fig. 1: area between the outer reef tract and the 30-fathom (55-m) isobath]. The broadest portions of the terrace are located in the southwest and northeast sectors of the platform, thus coinciding with the predominant orientation of winds, swells, and seas from the northwest, southwest, and northeast (7, 8).

We tried to determine whether the reefs originated by growth of coral or from consolidation of windblown sand. One section of outer reef tract lying south of the main island, in the area between Devonshire Bay (Fig. 1, *A*) and John Smith's Beach (Fig. 1, *B*), was selected for underwater study with SCUBA equipment during April 1966 (9). A profile (10) of the terrace in front of the reefs of this area (Fig. 2A) shows a nearly horizontal surface submerged to from 7 or 8 fathoms (13 to 15 m) near the base of the outermost reefs to about 10 fathoms (18 m) on the outer edge of the platform. Coral-encrusted blocks and mounds are distributed at large, with sand commonly ponded between them (Fig. 2B). The reef-front platform is commonly nar-

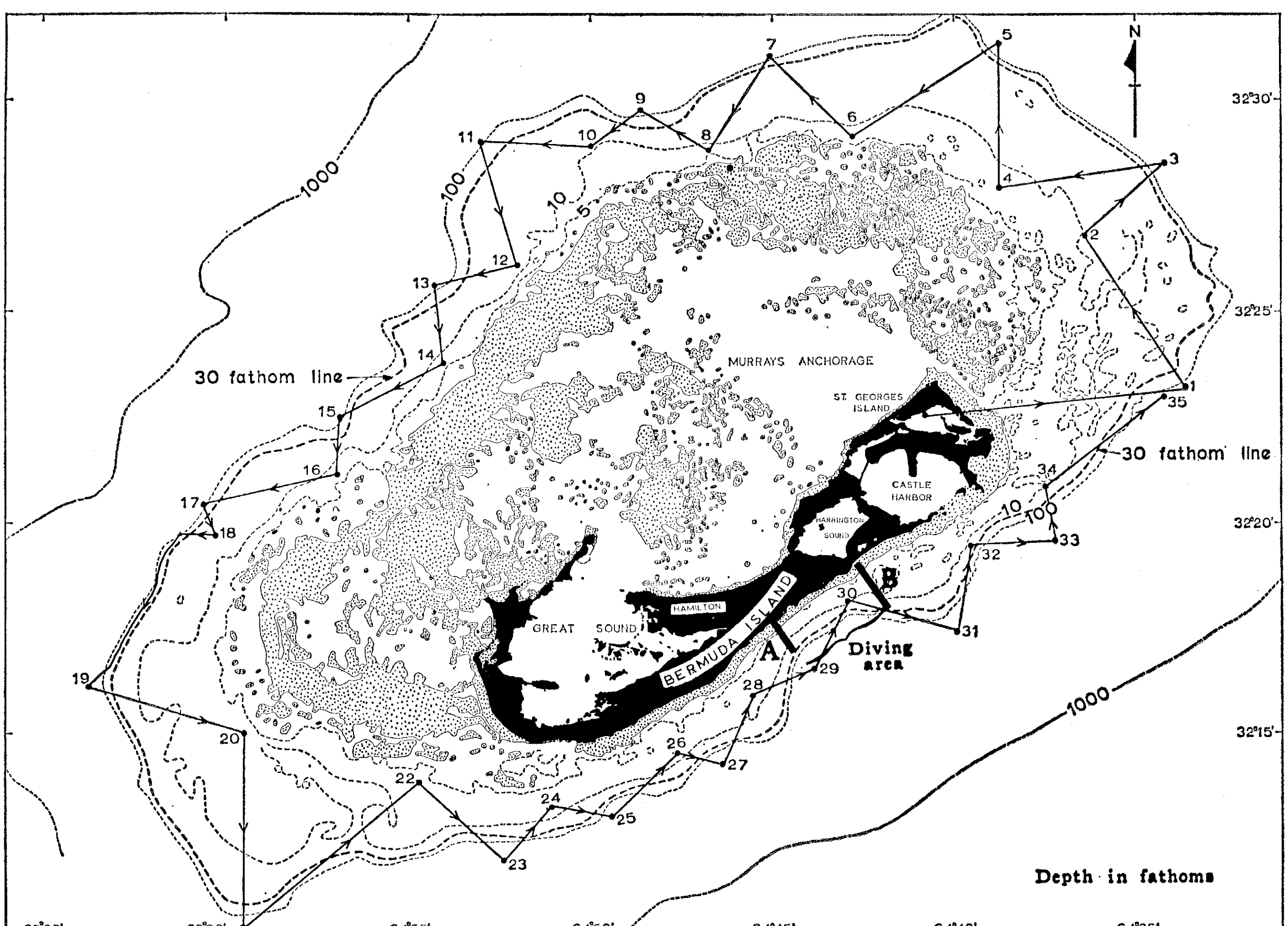

Fig. 1. The Bermuda platform and the area of reef investigated, southeast of the islands; *A*, Devonshire Bay; *B*, John Smith's Beach. Arrows indicate the track of C.N.A.V. *Sackville* in April 1966, and the locations of the bottom and subbottom profiles. Area between the outer reefs and the 30-fathom line is referred to as the reef-front terrace (1 fathom, 1.83 m).

rower than 2 km and may be as narrow as 1 km. The main reef tract is located several hundred to several thousand meters from the southern cliffs and roughly parallels them. The reefs on this part of the platform are discontinuous and considerably narrower than those in areas north of the islands.

The southeastern platform is considerably more exposed to open-sea conditions than are areas to the north, where the shallow, partially filled reef-lagoon reduces the effect of wave attack. As a result southern reefs and coastal margins bear the brunt of erosion. Waves generally attack the coast in a direction subnormal to the NE–SW trend of reefs and islands: from the southwest in late spring and summer and from other quadrauts during other seasons (*7*).

Under water the form of the reefs is unusual; some emerge and cause waves to break, especially at low tide. Most are relatively flat-topped and range in width from 10 to more than 100 m; their cliff-like margins are either perpendicular or, more often, overhanging (Fig. 3A). These steep walls of the reefs extend from the surface to a depth of 20 to 28 m in a series of step-like benches.

Particularly spectacular is the dissection of the reef by deep, linear, and irregular narrow passages encountered to depths as great as 23 m. Both open (Fig. 3A) and covered (Fig. 3B) grotto-like cavities are oriented subparallel to each other and occasionally normal to the coast. The irregular narrow winding passages, large cavities, and other reentries in the reef tract resemble morphological features that are exposed along the coastline.

Reefs appear as discontinuous oblong or circular masses; Agassiz (*11*) and others refer to some of those close to shore as "serpuline atolls," especially those appearing as rounded or crescent patches with raised rim and excavated, cup-shaped central parts. The rim of these particular isolated reef patches is exposed at low tide; it is formed by encrusting organisms including algae, serpulae, corals, barnacles, and other invertebrates. We found consolidated shell sand exposed on the upper margin of the more discontinuous flat-topped reef tract further from shore. Here the top of the reef rises to within 1 to 7 m of the surface and is relatively free of encrusting organisms and algae (Fig. 3C). Underwater observation shows that the terraced area seaward

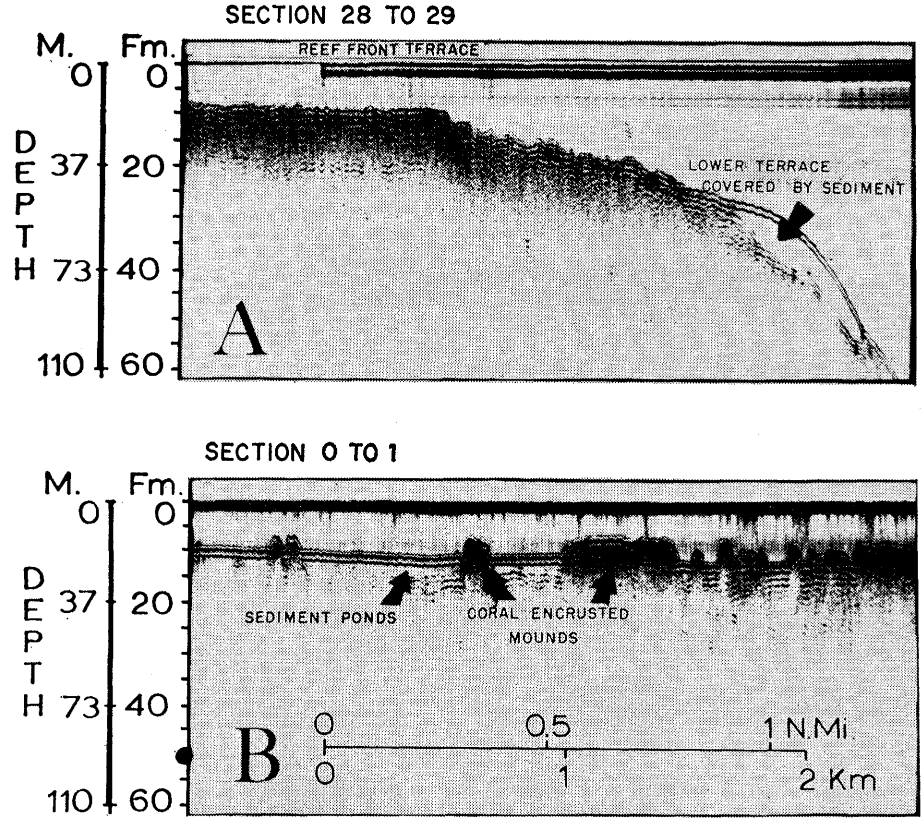

Fig. 2. Hydrosonde subbottom profiles (Fig. 1). (A) Truncated reef-front terrace and a lower sediment-covered terrace (*8*). Reef tract examined by divers is to the left of the profile. (B) Sediment ponds, consisting mainly of rippled sand and gravel, lying between coral-encrusted mounds on the reef-front terrace; note poor penetration and resolution in coral-encrusted aeolianite mounds on the reef-front terrace.

of the reefs tends to be somewhat more irregular than the almost-featureless surface recorded in some bottom and subbottom profiles.

Morphological forms produced or strongly modified by mechanical erosion are encountered on the reef tract; they include steep, overhanging reef walls (Fig. 3A), pinnacles (Fig. 4A), and smooth-scoured surfaces at the top (Fig. 3C) and at the base (Fig. 4B) of the reef. These features seem to have been produced by differential wear by abrasion, although biologic erosion of the type described by Neumann (*12*) also may have been effective to some degree. Large mounds encrusted with organisms, that lie adjacent to and beyond the main reef track, may represent blocks eroded from the reef tract.

Assemblages of corals, gorgonians, and other described (*1, 4, 8*) encrusting reef organisms coat almost the entire seaward cliff-like faces (Fig. 3A); the dark grottoes and honey-combed passages are only sparsely covered, however, and only in areas having sufficient light, such as near reentries (Fig. 3B).

Localized exposures of stratified sandstone occur in the reef. Poorly-to-well-consolidated, relatively well-sorted calcareous sandstone, collected on the exposed coral-free reef top and scoured base, and in narrow passages, was examined petrographically. The sandstone is made up largely of fresh-to-worn shell-sand material; it resembles in composition and texture the aeolianite (*3, 13*) that makes up most of the islands. These observations on morphology and composition clearly support the hypothesis (*4, 11, 14*) that the reef masses of Bermuda are not organically built mounds of the type found in tropic oceans, but submerged ridges of stratified windblown sand, only thinly encrusted with reef organisms.

These findings bear on the origin of the reef-front terrace that, like many other terraces of the world, lies at about 18 m (*15*). Two hypotheses are proposed for the origin of the terrace: (i) it is an old relict feature cut into the carbonate cap during earlier low stands by wave planation or by solution, or by both; or (ii) it is a recent phenomenon cut during the Holocene-Recent rise of sea level (*16*). Evidence supports both lines of reasoning.

Since submergence, mechanical and perhaps biologic erosion have modified, and are undoubtedly continuing to modify, the reef structure. We noted earlier the exposure of aeolianite and the lack of encrusting forms on the upper margins and within some reefs. Erosion of the aeolianite core is also prevalent, being indicated by the smoothly scoured base along much of the reef cliff in water as deep as 20 m or deeper.

During our dives in a relatively calm period, we felt the effect of surge motion only within 10 m of the surface and saw no movement of bottom sand at greater depth. Yet there is ample evidence that sediment is being actively deposited and moved at greater depths in the vicinity of the reef. Coarse, poorly sorted, cream-to-pink sand, sandy gravels, and gravelly sands floor the irregularities within and at the seaward base of the reef cliffs, between patch-like mounds on the reef-front terrace, and landward of the reef in the lagoon channel. Although shells and other forms of carbonate material are accumulating in depressions, most of the sand and coarser material is derived from wastage of the reef; the pink coloration, for instance, partly reflects the abundance of organisms such as the sessile foraminifer *Homotrema rubrum* that thrives in the shoal reef area (*17*). Coarse sand, sometimes to depths of 25 m, forms large ripples that generally lie normal to the smoothly scoured base of the reef. This fact suggests that most of the scouring and the movement of large ripples at depths beyond 10 m occurs intermittently during periods of rough weather, which are most frequent between November and March (*7*).

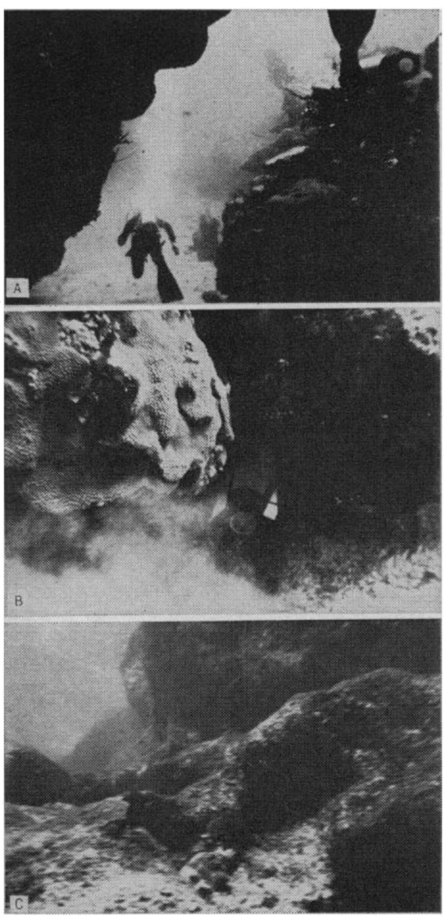

Fig. 3. (A) Reef-encrusted aeolianite reef-tract at a depth of about 17 m. Note overhanging reef margin and undercut reef base. Rippled coarse-grained sand floors the opening within the reef. Divers are swimming seaward to the reef-front terrace. (B) Grotto-like reentry within aeolianite reef core at a depth of about 13 m. Coral encrusting reef margin is absent within opening. Diver indicates scale. (C) Upper reaches of reef within zone affected by the surge. Note the lack of encrusting organisms, exposures of aeolianite, and waves breaking at surface (depth, about 5 m).

Some of the linear reentries and other irregularities in the reef, oriented subparallel to the direction of wave movement, may be effective as a natural breakwater system in dissipating wave energy in some way analogous to the biologically formed system of grooves and spurs in warmer waters where reef growth is more active (*18*, *19*). A similar situation prevails in a grooved zone cut in submerged wind-blown deposits at the inshore margin of some sectors of the Bahamas platform (*20*).

The reef-front terrace apparently is an older feature cut before the last rise in sea level. The peculiar honey-combed nature of the reef—especially the submerged grottoes—closely resembles caves, having partially collapsed roof structures, of the type observed on the island. These submerged cavities, most probably of solutional origin under subaerial conditions, were formed after consolidation of the belt-like accumulation of stratified wind-blown sand. Much of the reef tract surrounding the Bermuda platform and within the lagoon probably is of aeolianite origin—like the islands and the southern outer reefs. (*8*).

Isolated mounds distributed between the outer reef and the edge of the platform also appear to be erosional remnants of former more extensive aeolianite ridges that were eroded either by solution during lower stands of the sea or mechanically before and after the rise of sea level. Thus the morphology of the submerged platform is essentially a relict one.

Although coral growth has been marginal since the late Wisconsin and has not contributed substantially to the buildup of the reef, the thin veneer of encrusting organisms appears to have (i) retarded submarine erosion and wave planation of the aeolianite ridge, and (ii) provided some of the sediment lying in depressions around it. Our observations suggest that the wearing-back of reefs and the shoreward migration of the reef-front platform at the expense of the reef, even in this region that is generally unfavorable to reef growth, have been gradual in response to modern conditions.

So the preservation and only slight modification of the aeolianite ridge, and solutional features on the exposed

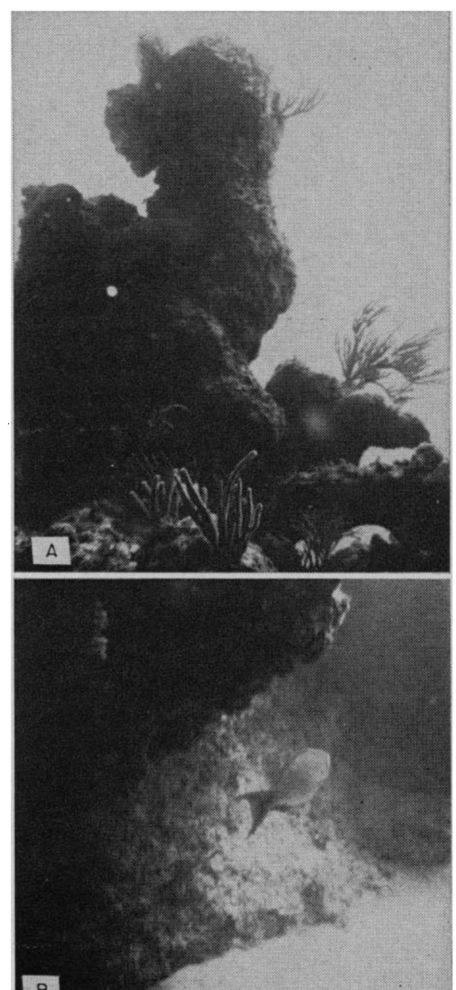

Fig. 4. (A) Sea fans, sea whips, and other organisms growing on a pinnacle about 1.5 m wide at a depth of about 7 m. (B) Seaward margin of the reef, showing smoothly scoured base of the reef cliffs; rippled sand is at a depth of about 20 m. Parrot fish in foreground.

and unprotected southeast margin of the Bermuda platform, strongly suggest that submarine planation has been a slow but not ineffective process. This conclusion may bear on inferred rates of truncation of reefs and oceanic atolls during recent periods of low stands of the sea in other areas of the world.

DANIEL J. STANLEY
Division of Sedimentology, Smithsonian Institution, Washington, D.C. 20560
DONALD J. P. SWIFT
Marine Biology Group, Puerto Rico Nuclear Center, Mayaguez

References and Notes

1. F. G. Walton Smith, *Atlantic Reef Corals* (Univ. of Miami Press, Coral Gables, Fla., 1948), pp. 37–39.
2. J. Rodgers, in *Regional Aspects of Carbonate Deposition*, R. J. LeBlanc and J. G. Breeding, Eds. (Soc. Econ. Paleontologists Mineralogists Spec. Publ. 5, Tulsa), p. 2.
3. R. W. Sayles, *Proc. Amer. Acad. Arts Sci.* **66**, 382 (1931); this and the two following references are the most complete summaries of the geologic history of Bermuda.
4. A. E. Verrill, *Conn. Acad. Arts Sci. Trans.* **12**, 45 (1907).
5. J. H. Bretz, *Bull. Geol. Soc. Amer.* **71**, 1729 (1960).
6. L. V. Pirsson, *Amer. J. Sci.* **38**, 189 (1914).
7. U.S. Navy Oceanog. Office, *Oceanographic Atlas of the North Atlantic Ocean* (Washington, D.C., 1963), sect. 4, pp. 1–227.
8. D. J. Stanley and D. J. P. Swift, *Program Ann. Meeting Geol. Soc. Amer. 1966*, p. 209; *Deep-Sea Res.*, in press.
9. Divers included H. Beals, M. G. Manktelow, F. Medioli, and the authors. All diving sections were made normal to the coast; they extended seaward from the rugged cliffs and shallow, submerged, and eroded coastal ledges, across the narrow sand-covered lagoon channel between reef and island, to the reefs and reef-front platform. Divers paid special attention to the contact area between the reef-front terrace and the reef tract.
10. Made with a Mark-IIA Hydrosonde, a 165-joule sparker.
11. A. Agassiz, *Amer. J. Sci.* **47**, 411 (1894).
12. A. C. Neumann, *Limnol. Oceanog.* **11**, 92 (1966).
13. F. T. MacKenzie, *Sedimentology* **3**, 52 (1964).
14. R. J. Nelson, *Geol. Soc. London Trans.* **5**, 103 (1837).
15. J. I. Tracey, Jr., H. S. Ladd, J. E. Hoffmeister, *Bull. Geol. Soc. Amer.* **59**, 861 (1948).
16. The most recent submergence probably began to cover the lower seaward margin of the reef [now shallower than 18 m, or close to the "10-fathom terrace" recognized in other areas (*15*)] about 8000 years ago, according to the sea-level curve in J. Curray, *The Quaternary of the United States*, H. F. Wright, Jr., and D. G. Frey, Eds. (Princeton Univ. Press, Princeton, N.J., 1965), fig. 2, p. 725; the curve shows a slight stillstand about that time.
17. F. T. MacKenzie, L. D. Kulm, R. L. Cooley, J. T. Barnhart, *J. Sediment. Petrol.* **35**, 265 (1965).
18. T. F. Goreau, *Ecology* **40**, 67 (1959).
19. E. Shinn, *J. Sediment. Petrol.* **33**, 291 (1963).
20. N. D. Newell, J. K. Rigby, A. J. Whiteman, J. S. Bradley, *Amer. Museum Nat. Hist. Bull.* **97**, 1 (1951); N. D. Newell, *Z. Geomorphol. Suppl.* **3**, 87.
21. We thank the Bermuda Biological Station for shore facilities; the officers and men of C.N.A.V. *Sackville* for efficient support offshore; the Institute of Oceanography, Dalhousie University, Halifax, N.S., and its director, G. Riley, for funds and equipment; and M. G. Gross, D. F. Squires (both of the Smithsonian Institution), and H. S. Ladd (U.S. Geological Survey) for critically reading the manuscript. A. E. Cok and L. Isham drew Figs. 1 and 2.

24 May 1967

Surveyor I: Location and Indentification

Abstract. *Surveyor I landed on the lunar surface on 2 June 1966 and obtained more than 11,000 pictures of the environment with its television camera. The same region was photographed by the 24-inch (61-centimeter) camera of Orbiter III on 22 February 1967. Surveyor I has been located in these Orbiter photographs; its image was found and all search and identification criteria were satisfied by the site.*

Surveyor I gathered extremely detailed information about the lunar surface in its immediate vicinity. Before this information could be extrapolated to other areas, viewed with lower resolution, the "ground truth" area of Surveyor had to be located and related to some category of characteristic surface.

Identification of Surveyor I in Orbiter III's photographs could enable direct comparison of the site, and possible correlation as to geology and terrain, with potential Apollo sites and additional Surveyor sites that were already defined in Orbiter's photographs across the lunar equatorial belt. Identification could also enable recommendation of other potential landing sites in terms of the statistical parameters characteristic of the distribution of craters with respect to number and size on the site of Surveyor I.

Surveyor I was approximately located by the spacecraft itself; the infor-

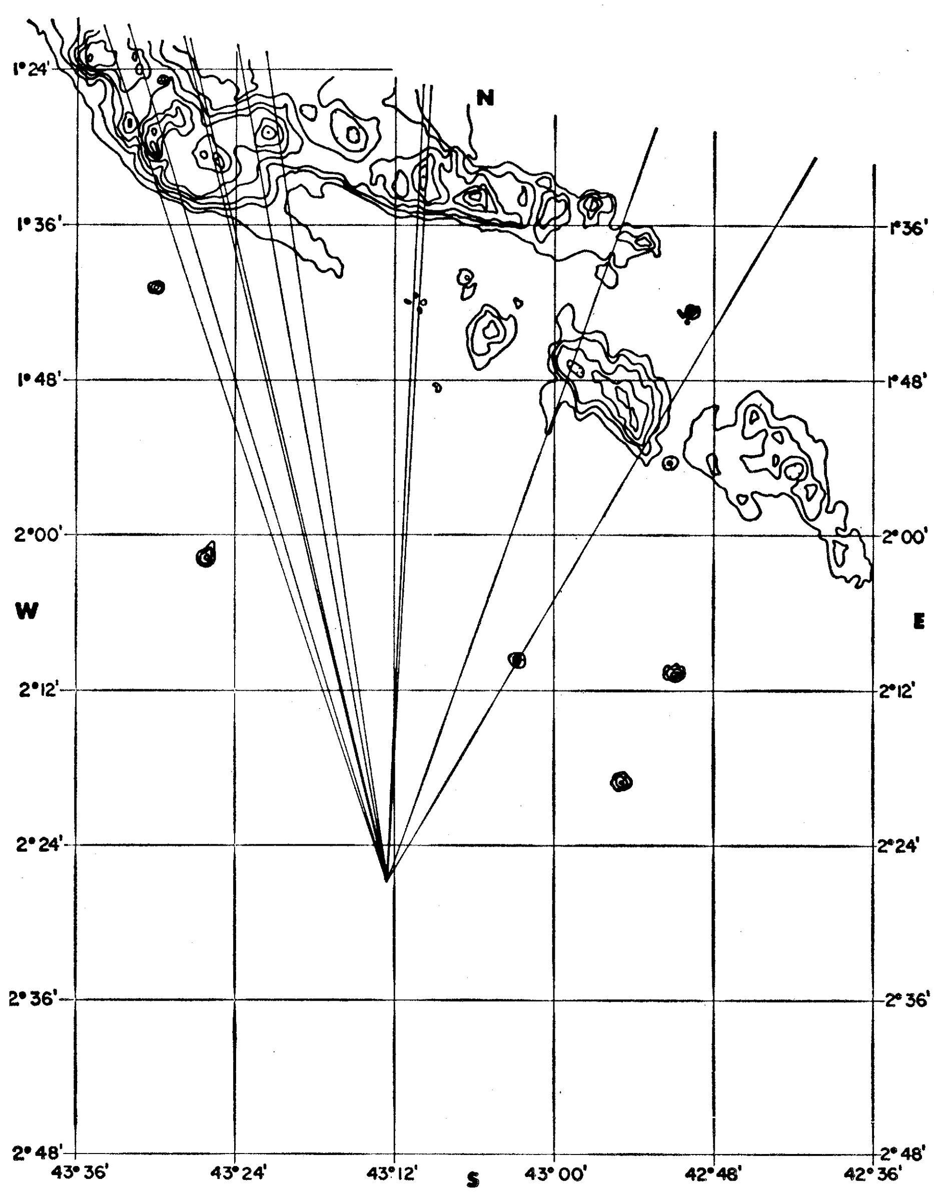

Fig. 1. Azimuthal projections from Surveyor I, superimposed over contours of low mountains to the north.